Computational Simulations of Fractional Flow Reserve Variability

Timur Gamilov[1,2,4], Philippe Kopylov[2,3], Sergey Simakov[1,2]

[1] Moscow Institute of Physics and Technology, Dolgoprudny, Russia
[2] Institute of Numerical Mathematics RAS, Moscow, Russia
[3] I.M. Sechenov First Moscow State Medical University, Moscow, Russia
[4] gamilov@crec.mipt.ru

Abstract. The value of fractional flow reserve (FFR) factor is the golden standard for making decision on surgical treatment of coronary vessels with multiple stenosis. FFR measurements require expensive minimally-invasive procedure using endovascular catheterization with ultrasound probe. In this work a non-invasive method of computational FFR assesmnent is considered. It is based on modelling 1D haemodynamics in patient-specific coronary region reconstruction using CT scans. Variability of computed FFR as a response to the change of vessels elasticity and autoregulation response rate is numerically studied.

1 Introduction

Multiple stenosis of coronary arteries is a common cardiovascular disease. It can cause myocard ischemia which frequently results in disability or death. Stenosis is usually treated with invasive endovascular intervention, i.e. stentng, or noninvasively by drugs therapy. Decision on type of treatment is based on the estimate of haemodynamical importance of the stenosis

The modern criterion of the coronary stenosis severity is fractional flow reserve (FFR) [6,7]. FFR is calculated as the ratio of mean pressure distal to stenosis to mean aortic pressure under conditions of vasodilator administration [6]. Values of FFR below 0.8 are associated with substantial haemodynamic importance of the stenosis and supported decision in favor of endovascular surgical intervention. The FFR based assessment allowed to reduce the number of costly operations as well as the number of incidences which caused disability or death [14].

Invasive measurements of FFR are regularly performed by endovascular ultrasound catheter and require fully operational catheterization laboratory. Modern methods of FFR estimate involve 3D blood flow modelling in the local region of the studied vessel [1,6]. This calculated value is usually referred to as computed FFR (cFFR) or virtual FFR. It requires complex simulations of local coronary region with high computational cost. Another approach is based on 1D blood flow modelling of coronary region [2,3,12]. One-dimensional approach allows to simulate substantial part of coronary region with multiple stenoses in different locations. The structure of computational domain can be obtained from patient's CT-scans [12].

Individual measurements of functional parameters such as vessel's elasticity and autoregulation response rate can't be measured routinely. In this work we propose computational approach for studying haemodinamical importance of the stenoses in a variety of possible conditions. So, 1D haemodynamics simulations [3] was used in this work to study variability of cFFR to changes of vessel wall elasticity and autoregulation response rate. Vessel wall elasticity and autoregulation response rate can change due to medications, lifestyle or aging [8]. This may increase or decrease FFR and, thus, severity of stenosis.

2 Methods

The model of blood flow in coronary vascular network considers unsteady viscous incompressible fluid flow through the 1D network of elastic tubes [11]. It takes into account patient-specific coronary arteries. Systemic circulation is simplified to a single large vessel. Veins are considered to have the same structure as arteries. The mode is supplemented by active vessel wall response (autoregulation) function according to [10]. In this section brief description of the model is presented, for details we refer to [3,10,12]. The flow in every vessel is described by mass and momentum balances

$$\partial A_k/\partial t + \partial(A_k u_k)/\partial x = 0, \tag{1}$$

$$\partial u_k/\partial t + \partial\left(u_k^2/2 + p_k/\rho\right)/\partial x = f_{fr}(A_k, u_k), \tag{2}$$

where k is the index of the vessel; t is the time; x is the distance along the vessel counted from the vessel junction point; ρ is the blood density (constant); $A_k(t,x)$ is the vessel cross-section area; p_k is the blood pressure; $u_k(t,x)$ is the linear velocity averaged over the cross-section; f_{tr} is the friction force. Wall-state equation is relationship between pressure and cross-section that defines elastic properties of the vessel wall

$$p_k(A_k) - p_{*k} = \rho c_k^2 f(A_k), \tag{3}$$

where $f(A)$ is monotone S-like function

$$f(A_k) = \begin{cases} \exp(\eta_k - 1) - 1, & \eta_k > 1 \\ \ln \eta_k, & \eta_k \leqslant 1, \end{cases} \tag{4}$$

p_{*k} is pressure in the tissues surrounding the vessel; c_k is the velocity of small disturbances propagation in the wall; $\eta_k = A_k/A_{0k}$; A_{0k} is the unstressed cross-sectional area. Parameter c_k defines elastic properties of the wall. High values of c_k correspond to stiff and rigid vessels, low values correspond to more soft and elastic vessels.

At the vessels junctions the Poiseuille's pressure drop condition is applied

$$p_k\left(A_k\left(t,\tilde{x}_k\right)\right) - p_{node}^l\left(t\right) = \varepsilon_k R_k^l A_k\left(t,\tilde{x}_k\right) u_k\left(t,\tilde{x}_k\right), k = k_1, k_2, \ldots, k_M, \tag{5}$$

To close the system we add the mass conservation condition and compatibility conditions of hyperbolic set (1),(2) (see [10]).

At the terminal point of the venous system ($x = x_H$) the pressure $p_H = 8mmHg$ is set as the boundary condition. At the entry point of the aorta the blood flow is assigned as the boundary condition

$$u(t,0)\,S(t,0) = Q_H\,(t)\,. \tag{6}$$

Here function $Q_H(t)$ for normal conditions corresponds to the heart rate value of 1 Hz and stroke volume of 65 ml [4] (see [3]).

The impact of autoregulation is important for the arterial vessels. We include it in the model as dependence of c_k in (3) on time-averaged pressure $\overline{p}_k$ [10]. c_k is updated every averaging period (one heart cycle)

$$\frac{c_{k,new}}{c_{k,old}} = \sqrt{\frac{\overline{p}_{k,new}}{\overline{p}_{k,old}}}, \tag{7}$$

where $\overline{p}_{k,new} = \dfrac{1}{(T_3 - T_2)l_k}\displaystyle\int_{T_2}^{T_3}\int_0^{l_k} p(x,t)dxdt$; l_k is the length of the k-th vessel; $\overline{p}_{k,old} = \dfrac{1}{(T_2 - T_1)l_k}\displaystyle\int_{T_1}^{T_2}\int_0^{l_k} p(x,t)dxdt$; T_1, T_2, T_3, T_4 are the initial moments of the successive averaging periods (successive cardiac cycles). Current value of c_k is calculated as

$$c_k = c_{k,old} + \gamma\frac{t - T_3}{T_4 - T_3}(c_{k,new} - c_{k,old}), \tag{8}$$

where $0 \leqslant \gamma \leqslant 1$ is the parameter reflecting the autoregulation response rate. $\gamma = 1$ corresponds to the normal autoregulation and $\gamma = 0$ — to the absence of autoregulation. Values between 0 and 1 can be associated with impaired autoregulation due to vessel wall malfunction or some drug administration.

An essential feature of coronary hemodynamics is compression of a part of coronary arteries during systole by myocard. This leads to the substantial perfusion during heart diastole [9]. Wall-state equation (3) is modified by setting $p_* = P_{ext}^{cor}\,(t)$. The shape of the function $P_{ext}^{cor}\,(t)$ is similar to the heart outflow time profile [3]. Maximum value is set to 120 $mmHg$ and 30 $mmHg$ for terminal vessels of left and right coronary artery, respectively. To simulate increased resistance we multiply R_k in (5) for all coronary vessels during systole by a factor of 3 [13].

2.1 Patient-specific 1D coronary network

The computational domain in a 1D network was generated on the basis of patient-specific data. Extraction geometry of coronary vessels from CT scans required complex image processing and segmentation algorithms described

in [3]. Segmentation algorithm uses Hough Circleness transformation and thresholding to find an initial mask, and Isopererimetric Distance Trees (IDT) algorithm to cut initial mask. Hessian based Frangi Vesselness filter is used for ostia points detection and small arteries segmentation. Then reconstruction of a topological structure of vessels is produced using thinning approach [12]. The result is the network of 1D vessels presented in Fig. 1.

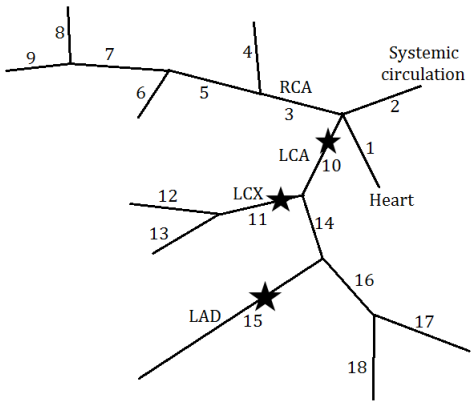

Fig. 1. The structure of reconstructed arterial part based on anonymous patient-specific data set. Stars designate stenoses. Parameters of the vessels are presented in Tab. 1

Table 1. Parameters of the arterial tree: k is the index of the vessel according to Figure 1, l_k is the length, d_k is the diameter, c_k is the stiffness (3), R_k is the resistance (5). Veins are considered to have the same structure with c_k lowered by 20 percent, d_k doubled.

k	l_k, cm	d_k, mm	$c_k, \frac{cm}{s}$	$R_k, \frac{ba \cdot s}{cm^3}$	k	l_k, cm	d_k, mm	$c_k, \frac{cm}{s}$	$R_k, \frac{ba \cdot s}{cm^3}$
1	5.28	21.7	1050	20	10	0.59	3.6	950	720
2	60.0	25.1	840	20	11	6.1	3.0	950	720
3	2.72	3.1	1200	7200	12	2.05	1.17	950	720
4	1.44	1.31	1200	7200	13	1.75	1.21	950	720
5	1.40	2.73	1200	7200	14	1.39	3.8	950	720
6	6.75	1.52	1200	7200	15	12.1	2.05	950	720
7	5.01	2.50	1200	7200	16	5.4	1.91	950	720
8	1.27	1.19	1200	7200	17	0.38	1.01	950	720
9	5.65	0.157	1200	7200	18	2.62	1.19	950	720

Patient was diagnosed with stenosis in three vessels: the proximal part (one third) of the left main coronary artery (LCA) with stenosis 55%, the middle one third of the left circumflex artery (LCX) with stenosis 80%, the middle one third of the left anterior descending artery (LAD) with stenosis 50%.

Stenosis was modelled by separating diseased vessel into three parts: stenosed part, proximal part and distal part [3]. Parameters of proximal and distal parts correspond to the parameters of the initial non-stenosed vessel. Parameters of stenosed part were modified as $S_{0_{stenosed}} = (1-\alpha)S_0$, $R_{stenosed} = \frac{l_{sten}}{l(1-\alpha)^2}R$, where α is the stenosis fraction, S_0 is the cross-section of initial vessel in the unstressed state, R is the resistance of the initial vessel, l is the length of the initial vessel, l_{sten} is the length of the stenosed part of the vessel. Parameter α was set in each case according to the above description.

3 Results

The cFFR is calculated as the ratio of average pressure in coronary artery distal to stenosis ($\overline{P}_{dist}$) to average aortic pressure ($\overline{P}_{aortic}$ — vessel 1 in Fig. 1) during vasodilator administration.

$$FFR = \frac{\overline{P}_{dist}}{\overline{P}_{aortic}}. \tag{9}$$

Vasodilator administration is simulated by doubling S_0 in the studied vessel and decreasing resistance R by the factor of 5. This method provided good agreement with experimental results according to [3].

Studying cFFR sensitivity to vessel wall elasticity involved calculating FFR with different values of parameter c_k (see (3)). All c_k were multiplied by a coefficient ϵ. $\epsilon = 1$ corresponds to c_k values from the Tab. 1. $\epsilon < 1$ corresponds to elastic vessels, $\epsilon > 1$ — rigid vessels. ϵ was varied from 0.4 to 2.0, which represents physiological range of parameter c_k. Two series of calculations were performed: first for the patient-specific case described in subsection 2.1; second for the increased stenosis in LAD up to 95 %. Results are presented on Fig. 2. It can be seen that biggest changes in FFR occur when ϵ is close to 1. Both extremely elastic and extremely stiff cases seem to have an asymptotic value of FFR. The valuable change of cFFR up to $\pm 5\%$ corresponds to the $\pm 20\%$ change of c_k.

Second part of this work is studying cFFR sensitivity to different autoregulation regimes. cFFR was calculated for different values of γ (see (8)) from 0 (absence of autoregulation) to 1 (normal autoregulation). All values of c_k are standard (see Tab. 1). Similarly to the previous simulations, two series of calculations were performed: first for the patient-specific case described in subsection 2.1; second for the increased stenosis in LAD up to 95%. Results are presented on Fig. 3. From fig. 3 it is clear, that cFFR value is highly

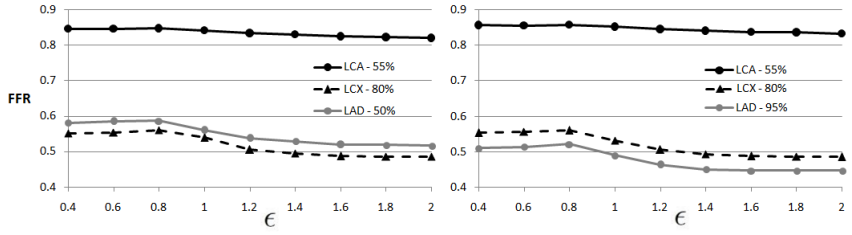

Fig. 2. Calculated FFR for different values of $c_k.c_k$ for all vessels were multiplied by ϵ. Left: patient-specific case (see Fig. 1); right: stenosis in LAD increased to 95%

variable for the values $\gamma < 0.5$ and almost not sensitive to the values of response rate $\gamma > 0.5$. Thus, we conclude that autoregulation with response rate corresponding to the $\gamma > 0.5$ become effective.

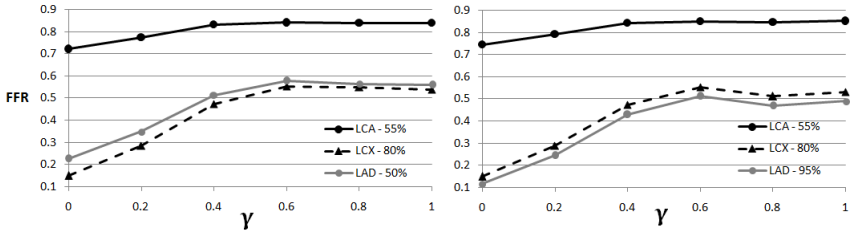

Fig. 3. Calculated FFR for different regimes of autoregulation (values of γ). $gamma = 1$ — normal autoregulation, $gamma = 0$ — absence of autoregulation. Left: patient-specific case (see Fig. 1); right: stenosis in LAD increased to 95%

Results demonstrate that FFR can vary substantially when some properties of vessel wall are changed. This is especially characteristic for autoregulation. Severe stenoses seem to have higher sensitivity to elasticity and autoregulation. We conclude that taking into account autoregulation is important when modelling coronary blood flow. Parameters c_k responsible for vessel elasticity should be approximated with precision better than 10% if we want to avoid significant errors in cFFR.

Increasing stenosis in LAD to 95% lead to the decrease of FFR in LAD but did not affect significantly other stenoses. The combined effect of multiple stenosed vessels and their mutual influence is an important question that lies beyond the subject of this work. Similar approach could be used to investigate the effect of different surgical strategies to find out which stenosis has the

biggest influence on perfusion. Potentially this could help to reduce the cost of treatment.

4 Discussion

Patient-specific data available in most of the clinics is very limited. As a result, some parameters of the models can not be defined with exact precision. It is important to investigate sensitivity of cFFR to such parameters. Results presented on Fig. 2 show that it is not necessary to know the value of c_k (Pulse Wave Velocity of unstressed vessel) should be defined with an error less than 10%. Such precision can be achieved without invasive procedures which allows to maintain relative simplicity in calculating cFFR.

Strictly speaking, cFFR values, which were simulated under activated autoregulation conditions ($\gamma = 1$), are not related to classic definition of invasively measured FFR. By definition, clinical FFR value is measured under vasodilator administration. From fig. 3 we may conclude, that clinically measured value of FFR may be underestimated. The further joint clinical and computational research in this field may increase precision of personal FFR assessment in realistic conditions.

Experimental studies show some correlation between FFR and age [5]. Aging has significant impact on elasticity of blood vessels [8]. There are many other factors that affect elastic and regulatory properties of vessel wall: sport, diet, medications, diseases, etc. This factors may affect severity of stenosis and thus sensitivity of FFR should be studied to prevent complications and derive recommendations for patients.

Acknowledgement The research was supported by Russian Science Foundation (RSF) grant 14-31-00024.

References

1. E.S. Bernad, S.I. Bernad, M.L. Craina, *Hemodynamic parameters measurements to assess the severity of serial lesions in patient specific right coronary artery*, Bio-Medical Materials and Engineering, **24(1)** (2014), 323–334.
2. E. Boileau, P. Nithiarasu, *One-Dimensional Modelling of the Coronary Circulation. Application to Noninvasive Quantification of Fractional Flow Reserve (FFR)*, Computational and Experimental Biomedical Sciences: Methods and Applications, **21** (2015), 137–155.
3. T.M. Gamilov, P.Y. Kopylov, R.A. Pryamonosov, S.S. Simakov, *Virtual fractional flow reserve assessment in patient-specific coronary networks by 1D hemodynamic model*, RJNAMM, **30(5)** (2015), 269–276.
4. W.F. Ganong, *Review of Medical Physiology*, Stamford, CT, Appleton and Lange, 1999.

5. H.S. Lim, P.A. Tonino, B. De Bruyne, A.S. Yong, B.K. Lee, Pijs N.H., W.F. Fearon, *The impact of age on fractional flow reserve-guided percutaneous coronary intervention: a FAME (Fractional Flow Reserve versus Angiography for Multivessel Evaluation) trial substudy.*, Int J Cardiol, **177(1)** (2014), 66–70.
6. P.D. Morris, D. Ryan,A.C. Morton, R. Lycett, P.V. Lawford, D.R. Hose, J.P. Gunn , *Virtual fractional flow reserve from coronary angiography: Modeling the significance of coronary lesions. Results from the VIRTU-1 (VIRTUal fractional flow reserve from coronary angiography) study*, JACC: Cardiovascular Interventions, **62** (2013), 149–157
7. L. Page, B. Riegel, S.B.K. Kern III, et. al., *ACC/AHA/SCAI 2005 Guideline update for percutaneous coronary intervention: A report of the American college of cardiology/American heart association task force on practice guidelines*, Journal of the American College of Cardiology, **47(1)** (2006), e1–e121.
8. R. Sala, C. Rossel, P. Encinas, P. Lahiguera, *Continuum of Pulse Wave Velocity from Young Elite Athletes to Uncontrolled Older Patients with Resistant Hypertension*, J. Hypertens, **28** (2010), pp 19.216
9. R.F. Schmidt, G. Thews, *Human Physiology.* volume 2, 2nd edition, Springer-Verlag Berlin Heidelberg, 1989.
10. S.S. Simakov, T.M. Gamilov TM, Y.N. Soe, *Computational study of blood flow in lower extremities under intense physical load* , RJNAMM **28(5)** (2013), 485–504.
11. S.S. Simakov, A.S. Kholodov, *Computational study of oxygen concentration in human blood under low frequency disturbances*, Math. Mod. and Comp. Sim. **1(2)** (2009), 283–295.
12. Yu.V. Vassilevski, A.A. Danilov, T.M. Gamilov, Yu.A. Ivanov, R.A. Pryamonosov, S.S. Simakov, *Patient-specific anatomical models in human physiology* , RJNAMM, **30(3)** (2015), 185–201.
13. M.A. Vis, P.H. Bovendeerd, P. Sipkema, N. Westerhof, *Effect of ventricular contraction, pressure, and wall stretch on vessels at different locations in the wall*, Am J Physiol Heart Circ Physiol, **272** (1997), H2963–H2975.
14. C.K. Zarins, C.A. Taylor, J.K. Min, *Computed fractional flow Reserve (FFTCT) derived from coronary CT angiography*, Journal of Cardiovascular Translational Research, **6(5)** (2013), 708–714.